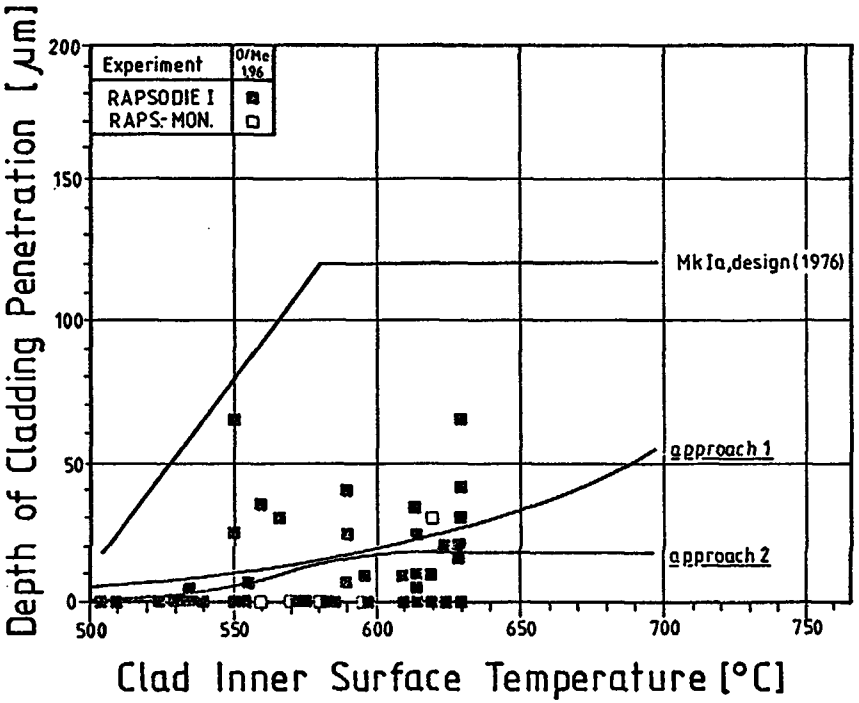

fig.2: Corrosion curves for O/Me = 1.96

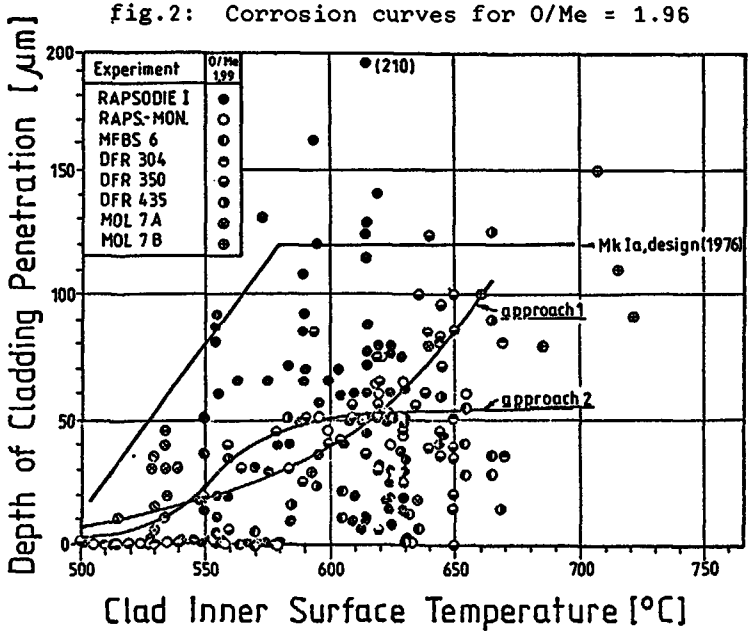

fig.3: Corrosion curves for O/Me = 1.99

Some Proposed Mechanisms for Internal Cladding Corrosion by M.H. Bradbury, S. Pickering, W.H. Whitlow, Euratom, presented by O. Götzmann, the Federal Republic of Germany.

ABSTRACT

In spite of extensive research during recent years, a comprehensive model for internal cladding corrosion in fast reactor oxide fuel pins has not yet been established. In this paper, a model is proposed which accounts for many of the features normally associated with this type of corrosion. The model is composed of a number of parts which describe the chronological sequence of events at the fuel/cladding interface. The corrosion reaction is visualised as being primarily chemical in character, involving the cladding steel, the fuel and the more aggressive fission products, notably caesium in the presence of oxygen. The model attempts to explain how corrosion starts, how it depends on the oxygen potential, why it occurs non-uniformly; also covered are phase changes within the cladding steel and morphological features such as the intergranular form of attack and the distribution of corrosion products in the fuel/cladding gap.

1. Introduction

At present, there is no generally agreed mechanism for the corrosion reaction at the inner surface of the cladding in LMFBR fuel elements. Nevertheless, a large body of experimental data exists and a number of important parameters affecting the reaction have been established. It is generally accepted that the corrosion reaction is the result of chemical and physical interations between the cladding steel (an austenitic stainless steel containing approximately 15% Cr/ 15% Ni, see Table 1), the fuel and certain fission products.

Composition of typical LMFBR cladding steel, DIN 1.4970 (in wt %)

C	Si	Mn	P	S	Cr	Ni	Mo	Co	Ti
0.10	0.43	1.51	0.05	0.07	15.02	14.91	1.18	≤0.07	0.40

Balance Fe

Table 1

Two types of attack have been observed, one confined mainly to the surface of the cladding, and the other (potentially the more serious) penetrating the steel cladding along grain boundaries. Attack usually occurs in an irregular manner over the inner surface of the cladding, and in the case of intergranular attack, its depth of penetration appears to vary markedly from site to site. Of the fission products, caesium above a critical oxygen potential is thought to be the most effective in promoting the intergranular type of attack and probably also the surface attack; tellurium, iodine, and selenium, either singly or in combination, are also effective in these respects. Temperature also appears to be very important; attack of the cladding steel has not been observed at temperatures much below about 550°C.

This report attempts to bring together a number of pieces of information, particularly in connection with caesium attack of the cladding steel, which have hitherto appeared to be isolated and to present these in terms of proposals for the reaction mechanism. These embody a number of novel ideas (based on thermodynamic arguments and experimental observations) developed recently in the Institute for Transuranium Elements. An attempt has been made to present the sequence of events in the corrosion process in chronological order, but it must be pointed out that some of the events almost certainly occur simultaneously. Literature and thermodynamic data supporting the model are presented along with the description in chapter 2. Additional experimental data are presented in the discussion (chapter 3).

2. The Proposed Reaction Sequence

Formation of protective oxides

1. Chromium oxide formation (Fig. 1)

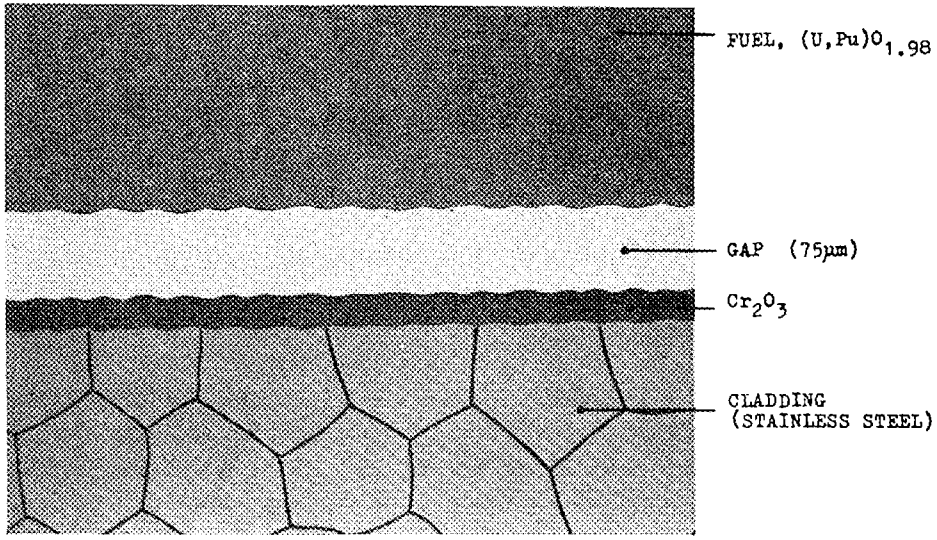

Fig. 1. Initial conditions

After fabrication, the inner cladding surface is likely to be covered with a very thin Cr_2O_3 type oxide (1). Normally, such oxides are only some 30 Å or so thick and are strongly adherent. The oxide is unlikely to be damaged mechanically during production of the fuel pin, but if this does occur, fresh oxide of the same type may be expected to form over the exposed metal, even though the production processes are performed in a relatively inert atmosphere (1).

2. Growth of chromium oxides at the inner cladding surface and oxygen redistribution in the fuel

Soon after reactor start-up, before significant amounts of fission products have been generated, the oxygen in the fuel (typical initial $\frac{O}{M} \simeq 1.98$) redistributes to create an $\frac{O}{M}$ ratio closely approximating to 2 at the outer fuel surface. The redistribution is believed to be rapid (≃48 h) (2), and thus the oxygen potential in the fuel/cladding gap is sufficient

for attack (see section 5) even before the fission products arrive in significant amounts.

The oxygen potential in the fuel/cladding gap ($\simeq$ - 100 kcal/mole O_2 at 700°C) is sufficient for further growth of the Cr_2O_3 type oxide on the inner cladding surface (oxygen pressure in equilibrium with chromium and Cr_2O_3 at 700°C is equivalent to -138 kcal/mole O_2). With the possible exception of carbon, impurities from the fuel and filler gas are not thought to be present in sufficient quantities within the fuel pin to affect the growth of the scale (3,4).

3. Local spinel formation (Fig. 2)

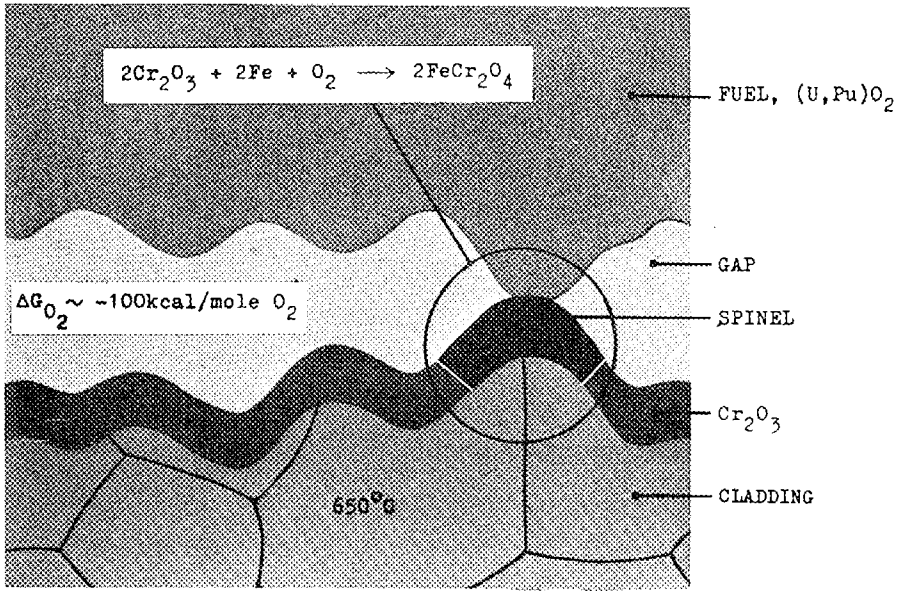

Fig. 2. Formation of spinel

It has been established that formation of Cr_2O_3 type oxide on stainless steels rapidly depletes the underlying steel in chromium. When the concentration of chromium at the steel/oxide interface reaches almost zero, the Cr_2O_3 type oxide is no longer in equilibrium with the underlying steel, and spinel type oxides begin to form (5). It is possible for these to form by reaction of iron with the Cr_2O_3 scale in the oxidising environment (5); thermodynamically such reactions may occur at oxygen potentials typical of those in a fuel pin (see Fig. 6 in section 6). Formation of spinel may occur at an early stage in the vicinity of surface defects (e.g. scratches) which by virtue of their geometric form can be more rapidly depleted in chromium due to oxide growth than a flat surface (6). In addition, spinel formation may be enhanced at places where the oxide scale has been abraded due to relative movement of the fuel and cladding during temperature cycles. This would expose freshly depleted steel to the (then) hot oxidising environment. Temperature is also believed to play an important role in determining the onset of spinel formation. Above $\simeq$ 700°C, appreciably greater quantities of spinel have been detected in the scale on stainless steels compared with those detected at 650°C under comparable conditions (7). It is interesting to note that Godesar (8) has predicted local increases in cladding temperature of as much as $\simeq$ 50°C due to direct contact between the fuel and cladding. Such increases are likely, therefore, to enhance spinel formation.

Thus, a surface defect, or more favourably a surface defect at a point where the temperature is above average may provide a site at which spinel formation will occur preferentially at an early stage. The location of fuel/cladding contact points will be random and will change with time (as a result of fuel relocation and temperature cycles) leading to random and changing sites which favour local spinel growth.

Arrival of fission products

4. Initial reactions of caesium (Fig. 3)

Caesium, tellurium and iodine are generally accepted as being the most aggressive of the fission products. Of these, caesium is of key importance because it is the most abundant

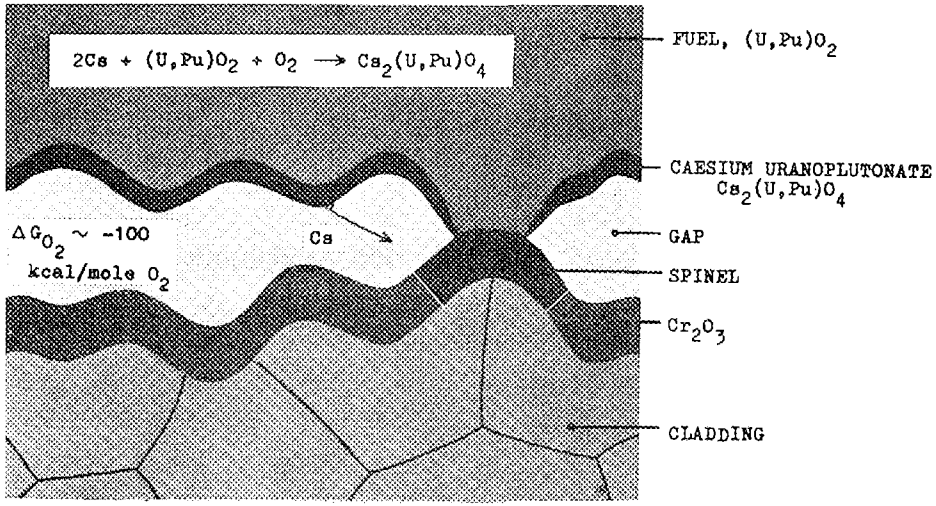

Fig. 3. Caesium uranoplutonate formation.

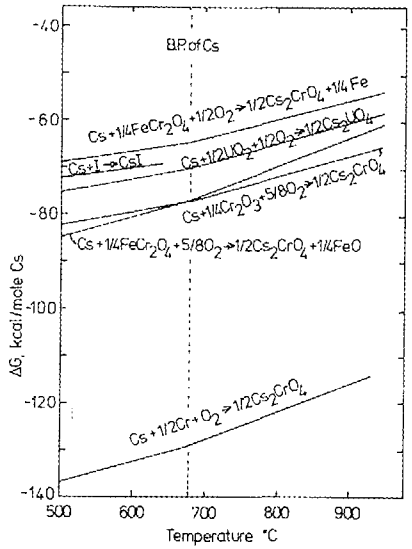

Fig. 4. Thermodynamic data relating to caesium containing compounds.

with a fission yield greater than that of tellurium and iodine by factors of 6 and 10 respectively. At sufficiently high caesium vapour pressures (see Fig. 4) caesium may react with tellurium and iodine to form the compounds caesium chalcogenide and caesium iodide which are believed to be less aggressive than their component element towards the cladding (9, 10, 11, 12).

Caesium (in the vapour state) will tend to migrate down any temperature gradient towards the cooler parts of the pin and also to the blanket. In these regions, it reacts to form caesium uranates or uranoplutonates (13) (Fig. 3). Such reactions of caesium with the fuel are believed to occur for all $\frac{O}{M} > 1.985$ and therefore, they may be expected to occur in fuel pins in which $\frac{O}{M} \simeq 2$ at the surface (14). Caesium uranates have been found to react with stainless steels only at oxygen potentials in excess of those expected in practice (15); it is reasonable to suppose that caesium uranoplutonates will behave in the same way. As a consequence of caesium uranate/uranoplutonate formation, therefore, most of the caesium is likely to be tied up and cannot react directly with the cladding. Nevertheless some caesium vapour will be present as a result of the vapour pressure of caesium over caesium uranate/uranoplutonate. It appears from Fig. 4 that this vapour pressure of caesium is so low that caesium iodide and probably caesium-tellurium compounds are not stable, so that iodine and tellurium are no longer bound to caesium and are thus free to react with the cladding. The reactions of iodine are discussed in section 12 and those of tellurium in section 7.

5. Susceptibility of oxide layer to caesium attack

In a fuel pin, caesium arriving at the inner surface of the cladding will be confronted with a layer of Cr_2O_3 type oxide containing regions of spinel (see section 3). It has been demonstrated that little or no reaction occurs between Cr_2O_3 and caesium in the presence of oxygen at partial pressures typical of those in an LMFBR fuel pin (16). There is experimental evidence, however, that a reaction occurs between caesium and stainless steel yielding caesium chromates above an oxygen potential threshold of -96 to -100 kcal/mole O_2 at 700°C (17, 18). In order to explain the initiation of

this reaction, i.e. the penetration of the oxide film, a reaction of caesium with the spinel type oxide is postulated. Thus, it is proposed here that caesium decomposes the spinel regions in the oxide film thereby permitting direct reaction of caesium (and the other fission products) with the steel in some places, while the rest of the cladding is still protected by a layer of Cr_2O_3 and that this localised breakdown of the spinel film is responsible for the observed non-uniform nature of cladding corrosion.

6. Decomposition of spinel (Fig. 5)

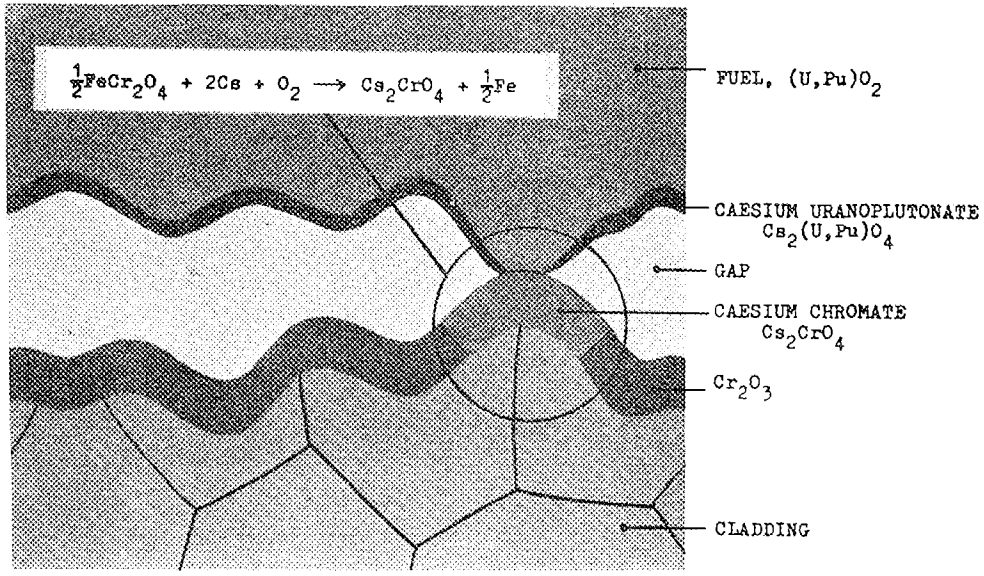

Fig. 5. Decomposition of spinel.

It is proposed that the regions of spinel in the oxide layer on the cladding surface are decomposed by a reaction of the following type:

a) $FeCr_2O_4 + 2x\ Cs + 2O_2 \longrightarrow 2\ Cs_x\ CrO_4 + Fe.$

If the oxygen potential is sufficient to oxidise iron to FeO, a variation of this reaction may occur:

b) $FeCr_2O_4 + 4\ Cs + \frac{5}{2}\ O_2 \longrightarrow 2\ Cs_2\ CrO_4 + FeO.$

At the oxygen potentials expected in practice, i.e. $\simeq$ -100 kcal/mole O_2, x may take the value 2, but other chromates are excluded on thermodynamic grounds (see Fig. 6) since the spinel $FeCr_2O_4$ would be unstable. The free energy changes associated with these reactions at 700°C are given also in Fig. 6.

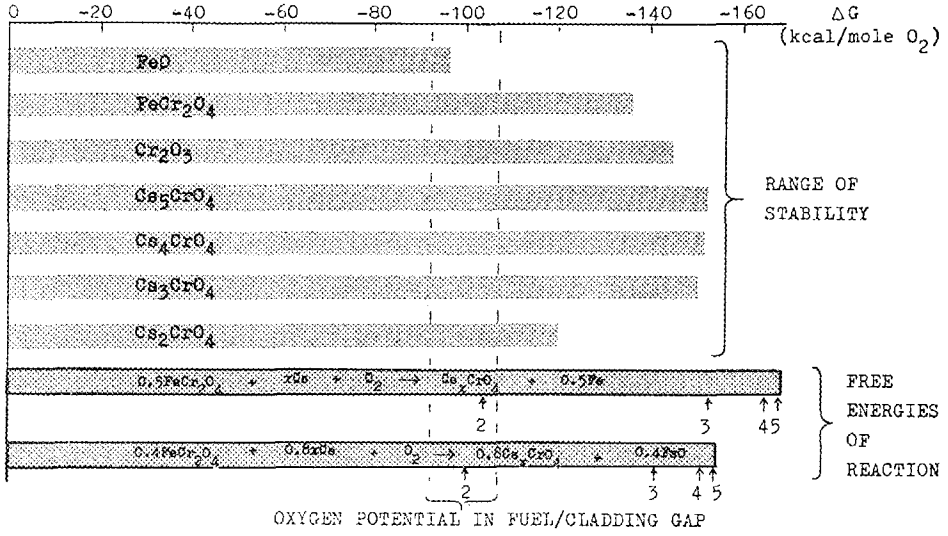

Fig. 6. Thermodynamic data relating to possible spinel decomposition reactions at 700°C.

It is interesting to note that the oxygen potential thresholds for the above reactions ((a) ~ 104 kcal/mole O_2 and (b) ~ 100 kcal/mole O_2) are close to the oxygen potential thresholds quoted in section 5 (-96 to -100 kcal/mole O_2, (17, 18)) for the reaction between stainless steel and caesium. It should be noted that in practice $FeCr_2O_4$ is believed to form from Cr_2O_3 + Fe + O (5) and thus its free energy of formation at 700°C is $\simeq$ -112 kcal/mole O_2.

It is proposed, therefore, that a reaction occurs between caesium vapour (see section 4) and spinel regions in the oxide layer according to reactions of the type given above. Only spinel regions in the oxide layer would be attacked and in consequence unprotected cladding would be exposed to attack only in certain places; subsequent attack would therefore be non-uniform.

7. Direct attack by fission products and location of the reaction front (Fig. 7)

Once the oxide layer has been penetrated, the fission products can be expected to react directly with the cladding steel. The corrosion reaction would be of the following type, assuming caesium to be the most abundant of the aggressive species (see Fig. 6 for free energies of formation of caesium chromates at 700°C):

$$x\,Cs + Cr + 2O_2 \longrightarrow Cs_x\,CrO_4.$$

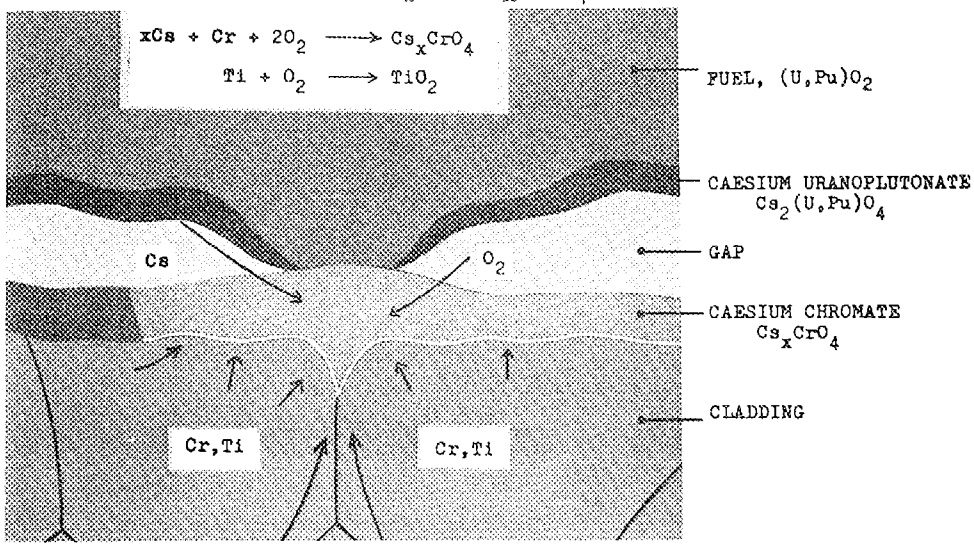

Fig. 7. Direct reaction of caesium with the cladding.

Tellurium may also be expected to react preferentially with chromium and manganese to form a telluride, the composition of which is reported to be Te 75%, Cr 20%, Mn 5% (19). The importance of this reaction may, however, be diminished by the tendency of tellurium to react with the fuel to form UOTe (14, 20).

The reaction site will depend on the relative rates of migration of the reactants; three possibilities exist:

a) outside the cladding in the reaction product layer, if the migration rate of chromium from the steel is greater than that of caesium from the fuel, resulting in caesium chromates in the fuel/cladding gap.

b) at the cladding surface, resulting in caesium chromates at the surface and possibly in open grain boundaries.

c) inside the cladding, if the migration rate of chromium in the steel is less than that of caesium and/or oxygen from the fuel into the steel, resulting in precipitates of caesium chromates in grain boundaries.

In practice, an oxygen gradient is likely to exist in the reaction product layer and surface regions of the cladding. Since the thickness of the reaction product and also the extent of attack within the surface regions of the cladding vary, it is extremely difficult to predict which of the caesium chromates are likely to form in any one position. Reactions may occur at more than one of the above sites (a, b, c) simultaneously and their locations may change with time if the relative migration rates of the reactants change due to the formation of precipitates, reaction product zones, etc.

8. Depletion of chromium in the cladding steel (Fig. 8)

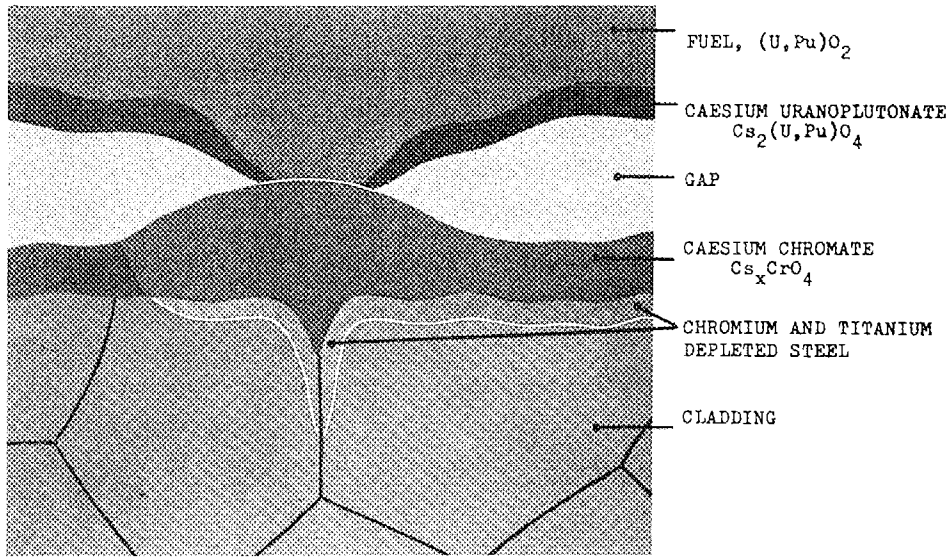

Fig. 8. Depletion of chromium and titanium in the cladding steel.

Whatever the location of the reaction site, the cladding will be depleted in chromium immediately below the inner surface and, because diffusion rates in grain boundaries are between 10^3 and 10^5 times faster than those in the bulk, depletion will also occur deep inside the cladding in regions adjacent to grain boundaries. Such depletion effects have been observed in irradiated cladding specimens by Electron Microprobe Analysis (21) and indirectly by metallography (22), in the latter case to depths of $\simeq 50\mu m$ below the cladding surface.

Effects due to depletion of chromium in the cladding steel

9. Transformation of austenite to BCC phase (Fig. 9)

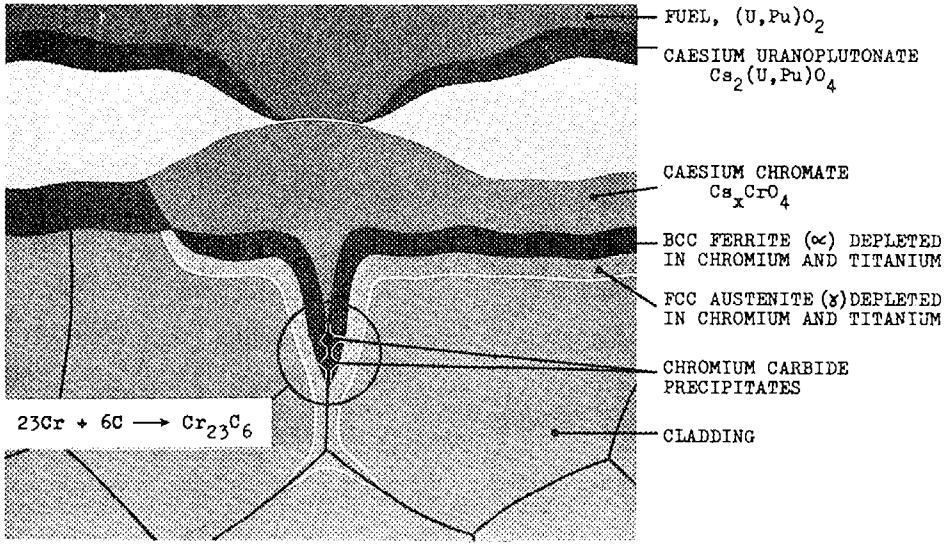

Fig. 9. Austenite (γ) → BCC phase (α) transformation and precipitation of chromium carbides.

It is possible for chromium depleted austenitic stainless steel of the type used for cladding applications in the LMFBR to undergo a phase change to a BCC structure, i.e. a ferrite-type structure, if the chromium content drops below a certain level, generally in the range 5 to 10 wt%, depending on the particular steel (23, 24).

The properties of the BCC phase will be different in several important respects to those of the FCC austenite from which it is formed. First, the diffusion rates of chromium, nickel and iron and probably oxygen are greater in the BCC phase than in the FCC austenite; for example, it is estimated that at 700°C, diffusion rates of chromium may be greater by a factor of $\simeq 40$ in the BCC phase compared with those in the FCC austenite (25, 26). Second, the solubility of carbon is likely to be much lower in the BCC phase than in the FCC austenite. The consequence of this solubility difference will be a rejection from the lattice of any carbon in excess of the solubility limit for the BCC phase. This effect is expected to occur in non-stabilised stainless steels but not to the same extent in stabilised stainless steels in which there is usually surplus stabilising element (titanium or niobium) which could take up at least some of the rejected carbon (see next section).

10. Chromium carbide formation in grain boundaries (Fig. 8 and 9)

In non-stabilised stainless steels, it is likely that chromium carbides ($Cr_{23}C_6$ will be considered, as this is the most commonly encountered carbide) will form in the grain boundaries due to thermal treatment of the steel. In addition, more carbides may form because of the rejection of carbon mentioned in section 9 above. Formation of such carbides removes more chromium from the steel, thereby promoting further transformation of the austenite to the BCC ferrite type phase (in steels of this particular type) and so making more carbon available, through carbon rejection to form more $Cr_{23}C_6$.

In stabilised stainless steels, thermodynamic arguments suggest that chromium carbide formation may result from oxidation of TiC or NbC. Kinetically this reaction would be more pronounced along and adjacent to grain boundaries.

$$23\ Cr + 6\ TiC + 6\ O_2 \longrightarrow 6\ TiO_2 + Cr_{23}C_6$$

$$\Delta G_{700^\circ C} = -\ 161\ \text{kcal/mole}\ O_2.$$

Electron Microprobe Analyses of simulation samples and irradiated cladding material have indicated a depletion of the stabilising elements Nb and Ti within the inter-granularly attacked zone (21) (stabilised austenitic stainless steels contain typically by weight, 0.4% Ti or 0.7% Nb, and 0.1% C). Because this destabilising reaction involves the formation of chromium carbides, it may result in further chromium depletion of the steel and thus promote the austenite to BCC phase transformation, as mentioned above in the case of non-stabilised steels.

11. Caesium attack on grain boundary carbides (Fig. 10)

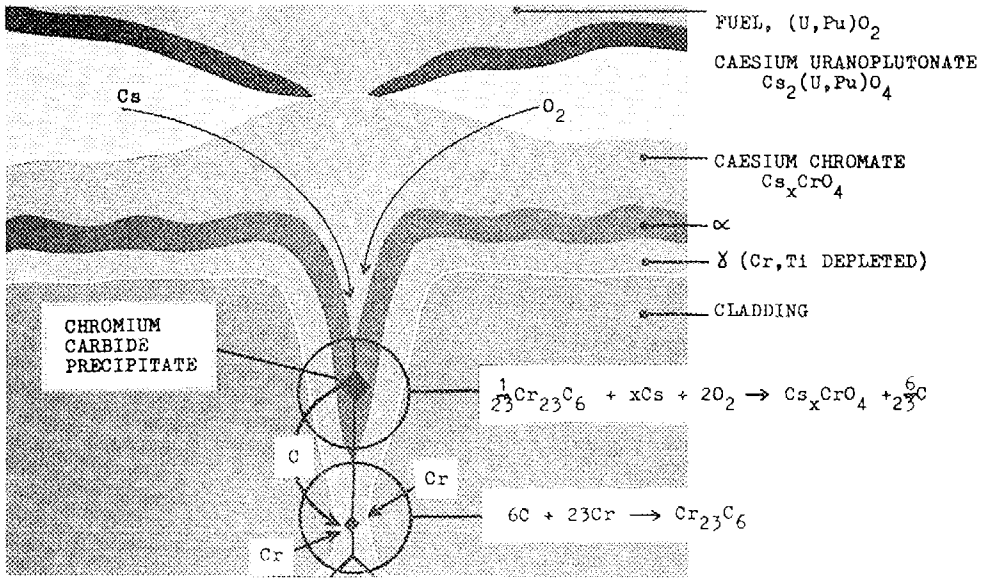

Fig. 10. Caesium attack on grain boundary carbides.

In principle, it is possible for caesium in the presence of oxygen to react with chromium carbide in the grain boundaries, thus:

(i) $\frac{1}{23}\ Cr_{23}C_6 + 4\ Cs + 2O_2 \longrightarrow Cs_4CrO_4 + \frac{6}{23}\ C$

$\Delta G_{700^oC} = -147$ kcal/mole O_2

Carbon released by this reaction may diffuse further into the cladding along grain boundaries, where it may react as follows:

(ii) $6C + 23\ Cr \longrightarrow Cr_{23}C_6$ $\quad \Delta G_{700^oC} = -18$ kcal/mole C.

Reaction (i) may be repeated, resulting in further attack along the grain boundary with the formation of more caesium chromate. Thus, carbon acts as a catalyst. However, the reaction may be limited by the availability of caesium and oxygen, since from (i) it follows that large quantities of both are required to react with each molecule of chromium carbide.

Disintegration of inner cladding surface and grain detachment

12. Attack involving iodine (Fig. 11)

As a result of reactions of the types described in the preceding sections, the surface and near-grain boundary regions of the cladding will be severely depleted in chromium, i.e. they will consist predominantly of the other major components of the steel, viz. iron and nickel. The surface of the cladding will be covered with a layer of corrosion products, consisting mainly of caesium chromates; the continuity of this layer may be disrupted through fuel/cladding mechanical interactions (see section 13) so that it will not act as an effective barrier to fission product species. Therefore, further significant reactions between the chromium depleted steel and fission products (including caesium as mentioned previously) are possible.

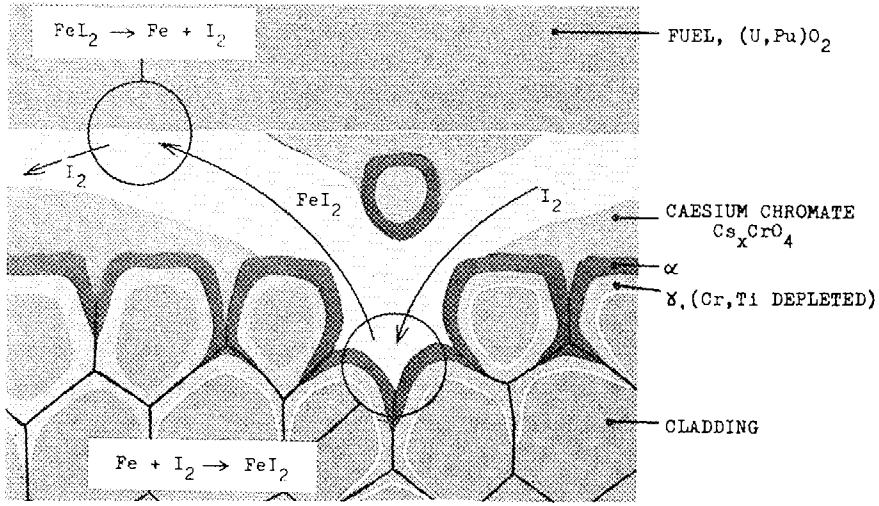

Fig. 11. Attack by iodine.

It has already been stated in section 4 that caesium can take part in a number of chemical reactions: it can react with the fuel to form caesium uranates and uranoplutonates, with the steel cladding to form caesium chromates and with other fission products to form, for example, chalcogenides. In principle, caesium can react also with iodine to form caesium iodide. However, the data presented in Fig. 4 indicate that both caesium uranates (and presumably caesium uranoplutonates) and the anticipated caesium chromates are more stable than caesium iodide.

Thus caesium should react preferentially with the fuel and depleted cladding material. The implication of this is that caesium iodide would be unstable (see Fig. 4).

The point in time at which direct reactions between gaseous iodine and the chromium depleted steel can occur via a van Arkel-de Boer type process will depend upon the availability of iodine in the fuel cladding gap. Calculation shows that if only 1% of the fission generated iodine remains in the free state, then the partial pressure of iodine will be sufficient to ensure the stability of, for example, iron iodide after only 0.5 a/o burn-up. At a relatively much later stage (11% burn-up), nickel iodide formation is also feasible.

Hence, iodide formation can lead to the removal of principally iron, nickel and other steel components from the chromium depleted regions.

The effect of iodine attack will then be an opening up of grain boundary regions followed by undercutting of the grains. This will seriously affect the mechanical integrity of the material in near surface regions such that whole grain detachment can occur, as observed in irradiated fuel pins. This reaction sequence offers an explanation for the presence of steel component elements, mainly iron and nickel, in the fuel/cladding gap adjacent to the fuel surface.

13. Fuel cladding mechanical interactions (Fig. 12a and b)

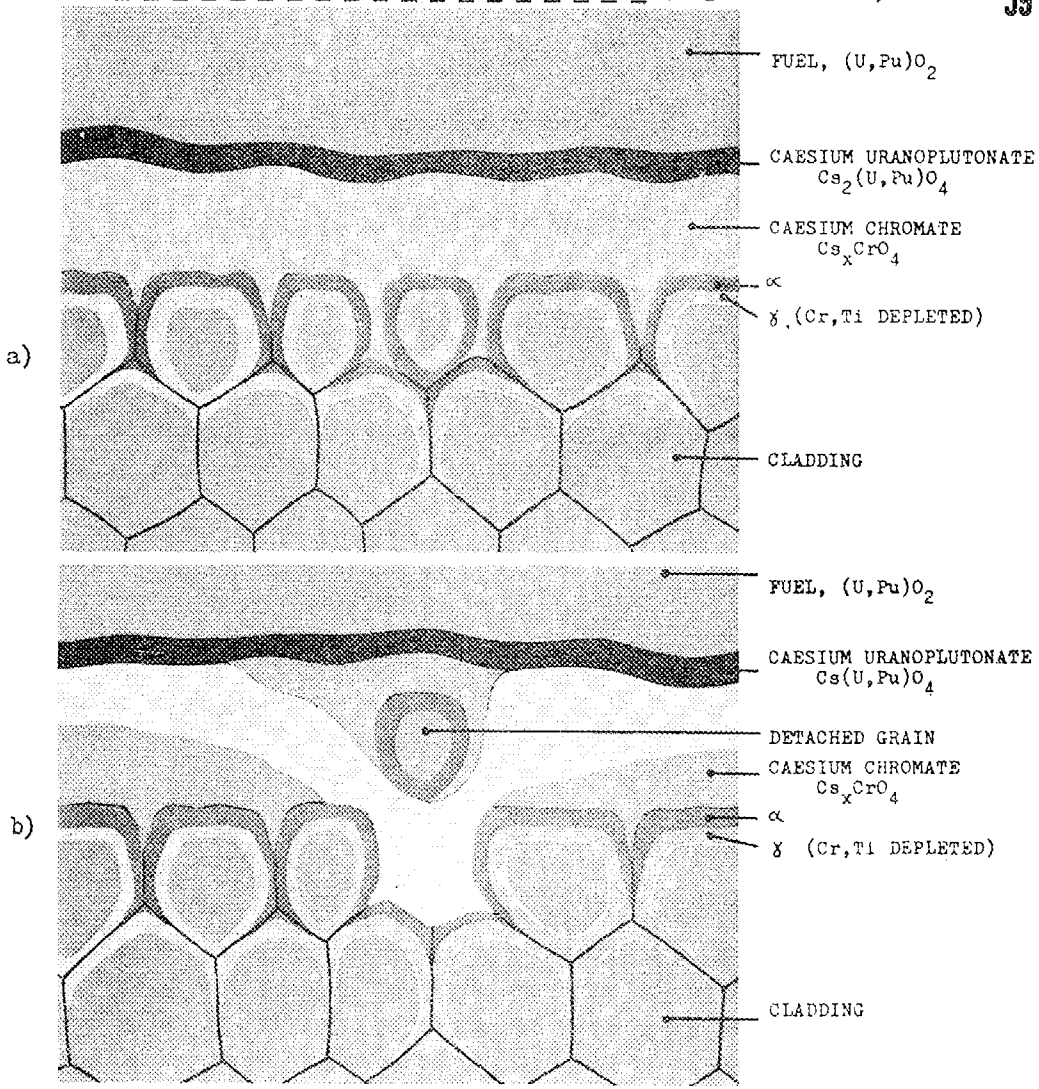

Fig. 12. Reactor power cycling : a) gap shut b) gap open

It is believed that whole grains of steel may be detached from the corroded inner cladding surface during reactor cycling. This can occur when the irradiation is sufficiently advanced for ceramic phases such as caesium chromates to be present in the fuel/cladding gap. Such phases are rather

plastic at operating temperatures and adhere to the fuel and the intergranularly attacked cladding surface. When reactor power is reduced, the fuel/cladding gap opens as a result of the different thermal expansivities of fuel and cladding. Because the ceramic phase in the gap adheres to both fuel and cladding, it exerts forces which oppose the opening of the gap. These forces may exceed the cohesive forces between the grains in the cladding surface when extensive intergranular attack has greatly reduced cohesion between grains. The result is that whole grains and sub-grains are detached from the cladding surface and are embedded in the ceramic phase in the gap. In post-irradiation micrographs, these detached grains are often observed as a sintered metallic band on the outer surface of the fuel.

3. Discussion of Supporting Evidence

Spinel type oxide formation

In short (100-200h) isothermal simulation experiments on cladding steels at temperatures of 700°C and above under oxygen potential conditions close to those expected in practice, the formation of spinel type oxides has been observed (7,27); in principal spinel can form at lower temperatures but for kinetic reasons the time required would be longer than that quoted above.

As stated previously, the earliest appearance of spinel is known to occur at surface defects such as scratch marks (6).

In the present model the predicted formation of spinel is expected to be enhanced by two in-pile phenomena listed below which act to increase the oxidation rate and thus favour chromium depletion and hence spinel formation.

(i) Fission fragment irradiation
Enhanced oxidation rates of up to 4.6 times normal due to fission fragment bombardment of austenitic stainless steel surfaces at 650°C have been reported (28, 29). Given a typical activation energy for oxidation in such steels of 58 kcal/mole O_2, an oxidation rate increase of 4.6 times is equivalent to a temperature increase of ≃ 50°C.

(ii) Fuel/cladding contact points
Calculations by Godesar (8) for typical current irradiation conditions indicate that the cladding temperature at a point of contact with the fuel can be ≃ 50°C above the temperature of an adjacent area which is separated from the fuel by a gas filled gap.

Caesium uranate / uranoplutonate formation

Post-irradiation examination, including electron microprobe analysis, of typical fuel pins has shown that caesium reacts both with the blanket (30, 31) and with the outer surface of the mixed oxide fuel (32, 33) to form what are believed to be caesium uranates/uranoplutonates. Fig. 13 shows the extent of this phase.

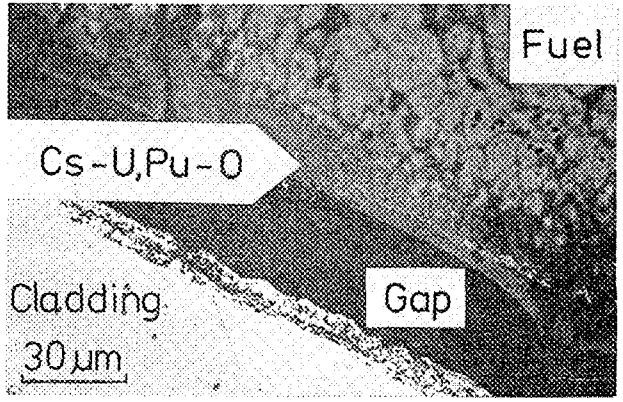

Fig. 13. Cs-(U,Pu)-O phase formed on the outside of a fuel pellet, initial $\frac{O}{M} = 1.98$, after ≃ 10 a/o burn-up in the Rapsodie reactor.

Preferential fission product attack on spinel type oxides

No direct evidence as yet exists to show that caesium reacts with spinel in preference to Cr_2O_3. It has, however, been demonstrated that Cr_2O_3 is resistant to attack by both

caesium (16) and tellurium (34) under the conditions of temperature and pressure expected in practice.

Simulation tests with caesium and bulk Cr_2O_3 in the temperature range 700-750°C showed that reaction was not detectable until the oxygen potential was far in excess of those expected in practice (16).

In the case of tellurium attack, it has been demonstrated by Robins (34) that when pre-oxidised stainless steel was exposed to tellurium vapour at 750°C, mounds of a tellurium rich phase formed only at cracks in the pre-formed chromium rich oxide layer. Regions of coherent oxide appeared to be unattacked.

Direct attack by caesium

A phase of constant composition containing caesium, chromium and oxygen has been detected by electron microprobe analysis in pins irradiated to ≃10% burn-up (35). This phase was found adhering to the corroded inner cladding surface and was interpreted as a product of a corrosive reaction of caesium with the stainless steel cladding. The composition of this phase corresponds most closely to $CsCr_3O_8$ rather than to any other known chromate: however, there exists some uncertainty in the formula since oxygen was determined by difference and it is well known that this can lead to significant errors. Chromates of the type Cs_2CrO_4 have been proposed as possible products of inner cladding corrosion (see chapter 2) and it is feasible that the chemical form of these could be changed in the surface of the specimen as a result of storage and specimen preparation.

Transformation of austenite (FCC) to a BCC phase

Electron microprobe analysis of corroded cladding has demonstrated unambiguously that chromium depletion of the cladding occurs in near surface regions, in regions adjacent to grain boundaries and particularly along the boundaries (35). (Fig. 14).

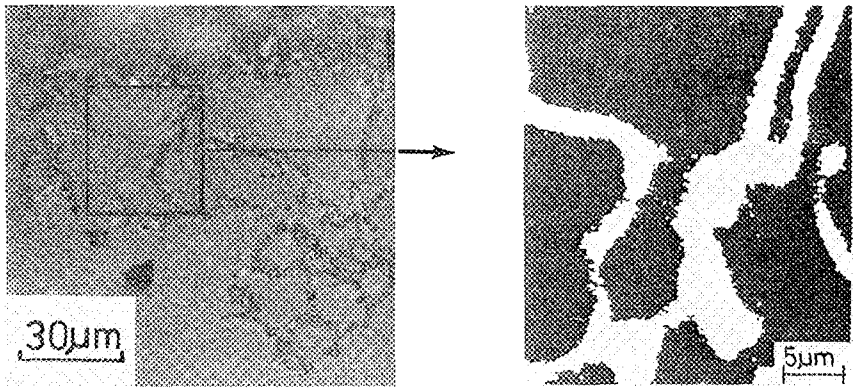

Fig. 14: The grain boundary phase revealed by interferometry (left) was shown by electron microprobe phase analysis (right) to contain 6-9 $^{W}/_{o}$ chromium compared with 15 $^{W}/_{o}$ in the bulk steel.

Chromium depletion is a prerequisite for a phase transformation from FCC to BCC in the cladding (23, 24) and a BCC phase has indeed been found by electron diffraction in the corroded regions of irradiated fuel pins (36); also, the specimens were strongly ferro-magnetic.

Corrosion simulation experiments (36, 37, 38) in which specimens of fully austenitic stainless steel were exposed to caesium were also found to contain a BCC phase (X-ray and electron diffraction) at the end of the test. This phase occurred adjacent to grain boundaries (Fig. 15). These experiments demonstrated that the austenite (FCC) → BCC phase transformation was induced by caesium attack since control experiments showed no transformation.

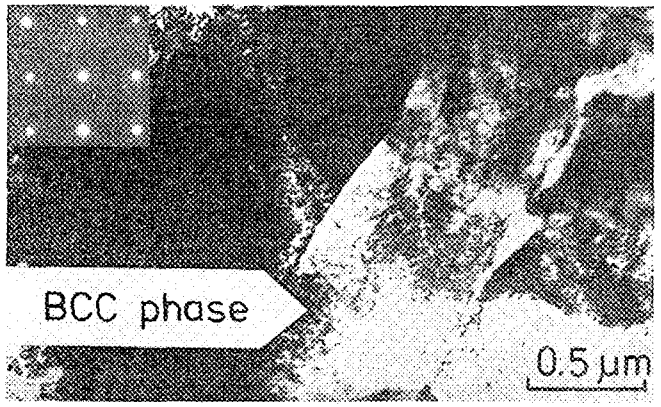

Fig. 15. Grain boundary BCC phase in caesium treated austenitic stainless steel as seen in T.E.M.

Loss of titanium and niobium from stabilised austenitic stainless steel and formation of chromium carbides

Electron microprobe analyses of corrosion simulation samples and irradiated cladding material have shown that the stabilising elements niobium and titanium can be depleted to depths of up to 50µm within the intergranularly attacked zone (21); losses of these elements of up to 55% were found (stabilised austenitic stainless steels contain typically by weight, 0,4% Ti or 0,7% Nb, and 0,1% C). In addition, titanium and niobium rich regions were detected in the fuel in irradiated specimens in quantities greater than could be accounted for by impurities or, in the case of niobium, fission (titanium is not a fission product).

Such losses of stabilising elements are expected to lead to the formation of chromium carbides of the type $Cr_{23}C_6$ and indeed $M_{23}C_6$ type carbides have been identified by electron diffraction in irradiated stabilised stainless steel samples in regions of intergranular attack (36) (Fig. 16).

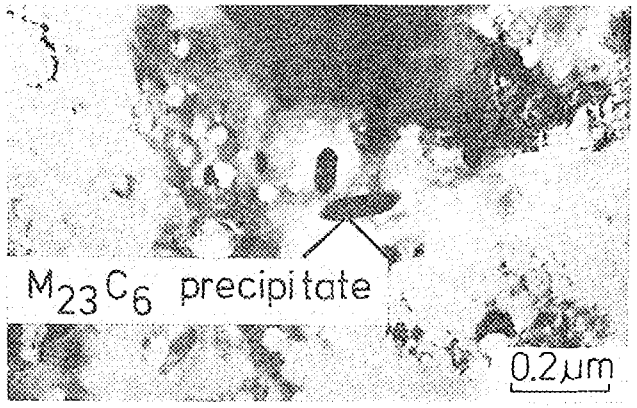

Fig. 16. Carbide precipitate, $M_{23}C_6$, in irradiated stabilised austenitic stainless steel.

Break-up of inner cladding surface

The proposed break-up of the corroded cladding surface by mechanical interaction between fuel and cladding is based on the appearance of the corrosion zone as seen in post-irradiation examinations. Fig. 17 shows a heavily corroded region which is not broken up (left); note the absence of ceramic phases in the gap. When ceramic phases are present, structures such as that on the right in Fig. 17 are normally seen.

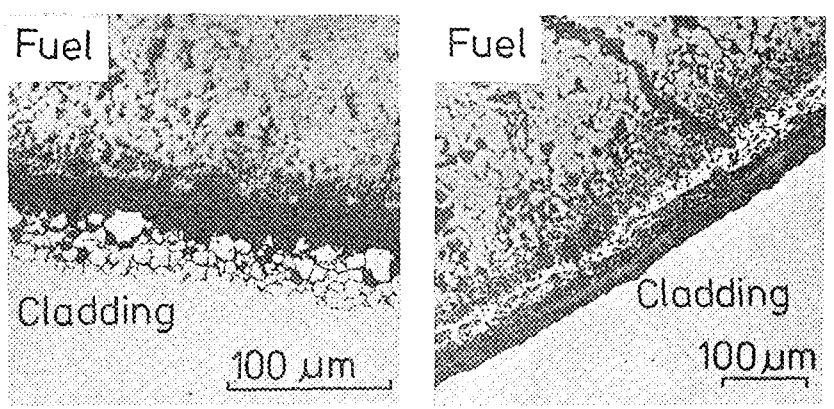

Fig. 17. Left - Intergranular corrosion without break-up of surface and no ceramic phase in gap.
Right - Ceramic phase in gap and detached band of cladding material.

Summary

The model offers explanations for the following features of inner cladding corrosion:

1) local and irregular depth of attack

2) oxygen potential threshold for attack

3) similar depth of intergranular attack in stabilised and non-stabilised cladding steels

4) morphology of the reaction product layer, in particular the iron-nickel metallic layer on the outer rim of the fuel

5) phase changes in the cladding steel.

Below are listed the new aspects and ideas contained in the model.

1) Local formation of spinel on the inner cladding surface, leading to local initiation of attack and subsequent irregular depths of attack.

2) Depletion of chromium and subsequent transformation of austenite to a BCC phase (ferritic type steel) especially along grain boundaries, as a result of chromium compound formation such as caesium chromates.

3) Depletion of the cladding steel stabilising elements, titanium or niobium, from stabilised steels, resulting in intergranular attack by a similar mechanism to that in non-stabilised steels.

4) Mechanical break-up, during reactor power cycling, of the cladding surface previously weakened by intergranular attack.

The model itself is limited in certain respects, as it must be at the present time, in view of the lack of key experimental data. For example, it is qualitative in character; no attempt has been made to explain the kinetics of inner cladding corrosion. It is assumed that the corrosion reactions are promoted mainly by caesium in the presence of oxygen, and while this fission product is regarded as being particularly effective in this respect, it is clearly an over-simplification not to consider in detail the roles of other aggressive species such as tellurium, etc. Some of the arguments introduced into the model are based on hypotheses and thermodynamic calculations and require experimental verification e.g. the direct reaction of caesium on spinel type oxides in the presence of oxygen. Such tests are under way as well as studies of the roles of other aggressive species in the corrosion reaction(s).

Acknowledgements

We would like to thank Drs. U. Benedict, I.L.F. Ray, C. Ronchi and C.T. Walker for making available results prior to publication. We would also like to thank M. S. Fourcaudot for performing many of the thermodynamic calculations.

References

1. W.H.J. Vernon, F. Wormwell and T.J. Nurse, Journal of the Iron and Steel Institute, 150(1944)81 A

2. C. Sari and B. Schumacher, J. Nucl. Mat., 61(1976)192

3. M.H. Bradbury, S. Pickering, C.T. Walker and W.H. Whitlow, EUR 5497/2(1976) (In Press)

4. M.G. Adamson and E.A. Aitken, GEAP 12533(1974)

5. W.H. Whitlow, Ph.D. Thesis, University of Bath, 1972

6. J.M. Francis and W.H. Whitlow, J. Nucl. Mat., 20(1966) 1.

7. O. Götzmann and P. Hofmann, KFK 1619, (1972)

8. R. Godesar, Proc. of Conf. on Physical Metallurgy of Reactor Fuel Elements, Berkeley, U.K., Sept. 1973, Published by the Metals Society London, 308

9. P.A. Maiya and D.E. Busch, Met. Trans. A, (1975) 409.

10. E.A. Aitken, M.G. Adamson and S.K. Evans, GEAP 12489,(1974)

11. E.A. Aitken, M.G. Adamson, D. Dutina, S.K. Evans and T.E. Ludlow, GEAP 12444 (1973)

12. W. Batey and K.Q. Bagley, J. Brit. Nucl. Energ. Soc. 13(1974)49

13. M. Coquerelle and S. Pickering, TUSR 20(1976)34

14. E.A. Aitken, S.K. Evans and B.F Rubin, IAEA-PL-463/16 (1974)275

15. O. Götzmann, P. Hofmann and F. Thümmler, J. Nucl. Mat., 52(1974)33

16. J.E. Antill, K.A. Peakall and E.F. Smart, Unpublished Results Harwell U.K. (1976)

17. P.A. Maiya and D.E. Busch, Met. Trans. A 64(1975)409

18. J.E. Antill, K.A. Peakall and E.F. Smart, AERE R7797 (1974)

19. D. Calais, M. Conte, F. de Keroulas and R. Le Beuze, IAEA-PL-463/17(1974)281

20. A.J. Klein Haneveld and F. Jellinek, J. Inorg. and Nucl. Chem., 26(1964)1127

21. C.T. Walker, To be Published

22. M. Coquerelle and S. Pickering, TUSR 20(1976)34 and TUSR 19(1975)37

23. W.H. Whitlow and R.K. Wild, Proc. of the BNES International Conference on Corrosion (1974)338

24. W.H. Whitlow, R.K. Wild and J.F. Norton, To be published

25. L.V. Pavlinov, E.A. Isadzanov and V.P. Smirnov, Fiz. Metalloved, 25(1968)959

26. C. Strawström and M. Hillert, Journal of the Iron and Steel Institute, 207(1969)77

27. I.L.F. Ray, C. Ronchi and W.H. Whitlow, To be published

28. M.J. Bennett, G.H. Chaffey and J.E. Antill, J. Nucl. Mat. 32 (1969) 299

29. M.J. Bennett and G.H. Chaffey, J. Nucl. Mat.55(1975)224

30. H.J. Powell, IAEA-PL-463/21 (1974)379

31. M. Coquerelle and S. Pickering, TUSR 18(1974)50

32. G.C. Giacchetti, TU Report 27/72 (1972)

33. D. Calais, R. Le Beuze and M. Conte, Trans ANS, 21(1975)186

34. I.H. Robins, Private Communication, (1977)

35. S. Pickering and C.T. Walker, TUSR 21(1976)43

36. I.L.F. Ray and C. Ronchi, To be published

37. R.W. Ohse and W.H. Whitlow, TUSR 18(1975) 53

38. U. Benedict and W.H. Whitlow, TUSR 20(1976) 40

Review and Evaluation of Cladding Attack of LMFBR Fuel by M. Koizumi, S. Nagai, H. Furuya, T. Muto, Japan.

Abstract

The behavior of cladding inner wall corrosion during irradiation was evaluated in the term of: fuel density, fuel form, O/M ratio, plutonium concentration, cladding composition, cladding pretreatment, cladding inner diameter, burn up and cladding inner wall temperature. Factors which influence are expected to be clare ~~are~~ O/M ratio, burn up, cladding inner diameter and cladding inner wall temperature. Maximum cladding inner wall corrosion depth was formulated as a function of O/M ratio, burn up and cladding inner wall temperature.

I. Introduction

The decrease of the cladding thickness due to the corrosion of fission products and their compounds is one of the important parameters to take into consideration for the fuel pin design. The cladding attack does not occur uniformly along the inner wall, and there have been two types of attack, intergranular attack and matrix attack. As the depths of this attack depend on the fuel O/M ratio, burn up, cladding inner wall temperature, etc, large scatterings have been observed in the measured values reported until now. The purposes of this paper are to evaluate the parameters affecting the cladding inner wall penetration depth and to derive the maximum cladding penetration depth as a function of O/M ratio, burn up and cladding inner wall temperature using reported data untill now and PNC data.